
Mn₃O₄-Graphene Hybrid as a High Capacity Anode Material for Lithium Ion Batteries

Hailiang Wang,^{†,§} Li-Feng Cui,^{‡,§} Yuan Yang,[†] Hernan Sanchez Casalongue,[†] Joshua Tucker Robinson,[†] Yongye Liang,[†] Yi Cui^{*,†} and Hongjie Dai^{*,†}.

[†]*Department of Chemistry and Laboratory for Advanced Materials, and* [‡]*Department of Materials Science and Engineering, Stanford University, Stanford, CA 94305, USA.*

[§] These two authors contributed equally to this work
hdai@stanford.edu and yicui@stanford.edu

Abstract We developed two-step solution-phase reactions to form hybrid materials of Mn₃O₄ nanoparticles on reduced graphene oxide (RGO) sheets for lithium ion battery applications. Mn₃O₄ nanoparticles grown selectively on RGO sheets over free particle growth in solution allowed for the electrically insulating Mn₃O₄ nanoparticles wired up to a current collector through the underlying conducting graphene network. The Mn₃O₄ nanoparticles formed on RGO show a high specific capacity up to ~900mAh/g near its theoretical capacity with good rate capability and cycling stability, owing to the intimate interactions between the graphene substrates and the Mn₃O₄ nanoparticles grown atop. The Mn₃O₄/RGO hybrid could be a promising candidate material for high-capacity, low-cost, and environmentally friendly anode for lithium ion batteries. Our growth-on-graphene approach should offer a new technique for design and synthesis of battery electrodes based on highly insulating materials.

Nanomaterials of metal oxides, such as Co₃O₄,^{1,2} SnO₂,³ FeO_x,⁴ and NiO¹ have been intensively studied as anode materials for lithium ion batteries (LIBs) aimed at achieving higher specific capacities than graphite. For instance, nanocrystals of Co₃O₄ have been synthesized for LIB anodes with specific capacities ~2X of that of graphite, affording LIBs with higher energy density.^{1,2} Compared to Co₃O₄, Mn₃O₄ is an attractive anode material for LIBs due to the high abundance of Mn, low cost and environmental benignity. However, little has been done thus far in utilizing Mn₃O₄ as an anode material^{5,6} partly due to its extremely low electrical conductivity (~10⁻⁷-10⁻⁸ S/cm) limiting its capacity ≤ ~400mAh/g even with Co-doping,⁶ well below the theoretical capacity of ~936mAh/g. It is highly desirable to increase the capacity of Mn₃O₄ by electrically wiring up Mn₃O₄ nanoparticles to an underlying conducting substrate.

Graphene is an excellent substrate to host active nanomaterials for energy applications due to its high conductivity, large surface area, flexibility and chemical stability. We have shown recently that the specific capacitance and power rate of Ni(OH)₂ could be enhanced by growing Ni(OH)₂ nanoplates on graphene sheets, useful for supercapacitor applications.⁷ Co₃O₄-graphene and Fe₃O₄-graphene composite materials have also been recently prepared as anode materials of LIBs,⁸ with comparable performance to previously reported Co₃O₄ and Fe₃O₄ based anodes.^{2a,2c,4a,4c} It is more challenging to explore Mn₃O₄-graphene hybrid materials due to the much lower conductivity of Mn₃O₄ than Co₃O₄ and Fe₃O₄. Here, we report a two-step solution phase method of growing Mn₃O₄ nanoparticles on graphene oxide (GO) to form a Mn₃O₄-reduced GO (RGO) hybrid material. The Mn₃O₄/RGO hybrid afforded an unprecedented high capacity of ~900mAh/g based on the mass of Mn₃O₄ (~810mAh/g based on the total mass of the hybrid) with good rate capability and cycling stability. This growth-on-graphene approach would be very useful in boosting the electrochemical performance of highly insulating electrode materials.

Mn₃O₄ nanoparticles were grown on GO sheets by a two-step solution phase reaction scheme [Figure 1, also see Supporting Information (SI) for details] recently developed for the synthesis of Ni(OH)₂/graphene hybrid.⁷ GO used in this work was prepared by a modified Hummers method (SI),⁹ in which a 6 times lower concentration of KMnO₄ was used (see SI) to result in GO sheets with lower oxygen content than Hummers' GO (~15% vs. ~30% measured by XPS and Auger spectroscopy).

In the first step, hydrolysis of Mn(CH₃COO)₂ in a GO suspension with a 10:1 *N,N*-dimethylformamide (DMF)/H₂O mixed solvent at 80 °C afforded dense and uniform coating with small and poorly crystalline precursor nanoparticles on GO (see SI and Figure S1). The mixed solvent and low temperature were important to control the hydrolysis reaction at a low rate to avoid particle formation in free solution. It is possible that nanoparticles grown this way were anchored covalently to GO through functional groups such as carboxyl, hydroxyl and epoxy groups on the surface of GO sheets.

The product from the first step was then transferred to de-ionized water and treated in hydrothermal conditions at 180 °C for 10 hours, which afforded well crystallized Mn₃O₄ nanoparticles uniformly distributed on RGO sheets (Figure 1), with ~10wt% RGO in the hybrid material. Through the synthesis, the starting GO sheets evolved into reduced graphene oxide due to the hydrothermal treatment at 180 °C, as evidenced by the red shift of the absorption peak in UV-Vis spectra (Figure S2).¹⁰ The size of the Mn₃O₄ nanoparticles was ~10-20nm as revealed by the scanning electron microscopy (SEM) and transmission electron microscopy (TEM) images (Figure 1b, 1d), which was consistent with the width of the diffraction peaks in XRD spectrum (Figure 1c). High resolution TEM image (Figure 1e) showed the crystal lattice fringes throughout the entire Mn₃O₄ nanoparticle formed on RGO.

The Mn₃O₄/RGO hybrid material was mixed with carbon black and polyvinylidene fluoride (PVDF) in a weight ratio of 80:10:10 for preparing a working electrode. The electrochemical measurements were carried out in coin cells with a Li foil as the counter electrode and 1M LiPF₆ in 1:1 ethylene carbonate (EC) and diethyl carbonate (DEC) as the electrolyte. Figure 2a showed the charge and discharge curve of Mn₃O₄/RGO anode for the first cycle at a current density of 40mA/g and cycled between 3.0V-0.1V vs Li⁺/Li. The capacity corresponding to the voltage range of ~1.2-0.4V of the first Li⁺ charge curve was due to irreversible reactions between Li⁺ and RGO and

decomposition of the electrolyte solvent forming a solid electrolyte interphase (SEI).¹¹ The voltage plateau at ~0.4V reflected the Li⁺ charge reaction: $\text{Mn}_3\text{O}_4 + 8\text{Li}^+ + 8\text{e}^- \rightarrow 3\text{Mn(0)} + 8\text{Li}_2\text{O}$.^{8b} The discharge curve showed a sloping plateau at ~1.2 V due to the reverse reaction. After several conditioning cycles, the Coulombic efficiency of the coin cell increased to higher than 98% (Figure 2b, 2c), indicating good reversibility of the above conversion reaction between Mn₃O₄ and Mn(0). The charge capacity in the range of 1.2-0.4V was mainly due to reduction from Mn(III) to Mn(II), and the 0.4-0.1V range reflected the reduction from Mn(II) to Mn(0).⁶ Little charge capacity would be obtained in the range of 1.2-0.5V if the electrode was cycled between Mn(II) and Mn(0).⁶ This further verified the conversion reaction we suggested above.

Figure 2b showed representative charge and discharge voltage profiles of the Mn₃O₄/RGO anode at various current densities (see Figure S4 for other data sets). With the increase of current density, the charge potential of Mn₃O₄/RGO anode decreased and the discharge potential increased rendering higher overpotential. The cell was first cycled at a low current density of 40mA/g for 5 cycles, where a stable specific capacity of ~900mAh/g (Figure 2c) was obtained based on the mass of the Mn₃O₄ nanoparticles in the Mn₃O₄/RGO hybrid (~810mAh/g based on the total mass of the hybrid), which was very close to the theoretical capacity of ~936mAh/g for Mn₃O₄ based on the conversion reaction above. This is also the highest capacity that has been reported for Mn₃O₄ anode materials. To our knowledge, previously, the highest capacity with similar cycle stability for Mn₃O₄ anode was ~500mAh/g at ~33-50mA/g.⁶ Our Mn₃O₄ nanoparticles formed on RGO showed good rate performance as well. The capacity was as high as ~780mAh/g after we increased the current density by 10 times. Even at a high current density of 1600mA/g, the specific capacity was ~390mAh/g, still higher than the theoretical capacity of graphite (~372mAh/g). A capacity of ~730mAh/g at 400mA/g was retained after 40 cycles of charge and discharge at various current densities (Figure 2c), indicating good cycling stability (cycling data up to 150 cycles available in Figure S4).

The high capacity and rate capability, and good cycling stability of our Mn₃O₄/RGO hybrid material were attributed to the intimate interaction between the graphene substrates and the Mn₃O₄ nanoparticles directly grown on them, which made Mn₃O₄ electrochemically active since charge carriers could be effectively and rapidly conducted back and forth from the Mn₃O₄ nanoparticles to the current collector through the highly conducting three-dimensional graphene network. The graphene-nanoparticle interaction also afforded a good dispersion of the Mn₃O₄ nanoparticles grown on the RGO sheets to avoid aggregation (Figure S5), desired for cycle stability.

In a control experiment, we synthesized free Mn₃O₄ nanoparticles by the same two-step method without any graphene added (SI). Although the free Mn₃O₄ nanoparticles had similar morphology, size and crystallinity as those formed on RGO sheets (Figure S3), the electrochemical performance of these free Mn₃O₄ nanoparticles physically mixed with carbon black was much worse than the Mn₃O₄/RGO hybrid material mixed with carbon black. At a low current density of 40mA/g, the free Mn₃O₄ nanoparticles showed a capacity lower than 300mAh/g, which further decreased to ~115mAh/g after only 10 cycles (Figure 2d).

In conclusion, by selectively growing Mn₃O₄ nanoparticles on graphene oxide to form Mn₃O₄/RGO hybrid, we enabled Mn₃O₄ approaching its theoretical capacity as an anode material for LIBs. The Mn₃O₄-graphene hybrid could be further explored for high-capacity, low-cost and non-toxic anode material for battery applications. Our growth-on-graphene approach should also offer an effective and convenient technique to improve the specific capacities and rate capabilities of highly insulating electrode materials in the battery area.

Acknowledgement. This work was supported in part by Office of Naval Research and KAUST Investigator Award.

References

- (1) Poizot, P.; Laruelle, S.; Grugeon, S.; Dupont, L.; Tarascon, J.-M. *Nature* **2000**, *407*, 496-499.
- (2) (a) Nam, K. T.; Kim, D. P.; Yoo, J.; Chiang, C.; Meethong, N.; Hammond, P. T.; Chiang, Y.; Belcher, A. M. *Science* **2006**, *312*, 885-888; (b) Lou, X. W.; Deng, D.; Lee, J. Y.; Feng, J.; Archer, L. A. *Adv. Mater.* **2008**, *20*, 258-262. (c) Li, Y.; Tan, B.; Wu, Y. *Nano Lett.* **2008**, *8*, 265-270.
- (3) (a) Meduri, P.; Pendyala, C.; Kumar, V.; Sumanasekera, G. U.; Sunkara, M. K. *Nano Lett.* **2009**, *9*, 612-616; (b) Ye, J.; Zhang, H.; Yang, R.; Li, X.; Qi, L. *Small* **2010**, *6*, 296-306.
- (4) (a) Ban, C.; Wu, Z.; Gillaspie, D. T.; Chen, L.; Yan, Y.; Blackburn, J. L.; Dillon, A. C. *Adv. Mater.* **2010**, *22*, E145-E149; (b) Zhong, J.; Cao, C.; Liu, Y.; Li, Y.; Khan, W. S. *Chem. Commun.* **2010**, *46*, 3869-3871. (c) Wang, S.; Zhang, J.; Chen, C. *J. Power Sources* **2010**, *195*, 5379-5381.
- (5) Fan, Q.; Whittingham, M. S. *Mater. Res. Soc. Symp. Proc.* **2007**, *972*, 0972-AA07-03-BB08-03.
- (6) Pasero, D.; Reeves, N.; West, A. R. *J. Power Sources* **2005**, *141*, 156-158.
- (7) (a) Wang, H.; Robinson, J. T.; Diankov, G.; Dai, H. *J. Am. Chem. Soc.* **2010**, *132*, 3270-3271; (b) Wang, H.; Sanchez Casalongue, H.; Liang, Y.; Dai, H. *J. Am. Chem. Soc.* **2010**, *132*, 7472-7477.
- (8) (a) Yang, S.; Cui, G.; Pang, S.; Cao, Q.; Kolb, U.; Feng, X.; Maier, J.; Mullen, K. *ChemSusChem* **2010**, *3*, 236-239; (b) Wu, Z.; Ren, W.; Wen, L.; Gao, L.; Zhao, J.; Chen, Z.; Zhou, G.; Li, F.; Cheng, H. *ACS Nano* **2010**, *4*, 3187-3194. (c) Zhang, M.; Lei, D.; Yin, X.; Chen, L.; Li, Q.; Wang, Y.; Wang, T. *J. Mater. Chem.* **2010**, *20*, 5538-5543. (d) Zhou, G.; Wang, D.; Li, F.; Zhang, L.; Li, N.; Wu, Z.; Wen, L.; Lu, G. Q.; Cheng, H. *Chem. Mater.* **2010** ASAP. DOI: 10.1021/cm101532x.
- (9) (a) Hummers, W. S.; Offeman, R. E. *J. Am. Chem. Soc.* **1958**, *80*, 1339-1339; (b) Wang, H.; Wang, X.; Li, X.; Dai, H. *Nano Res.* **2009**, *2*, 336-342; (c) Sun, X.; Liu, Z.; Welscher, K.; Robinson, J. T.; Goodwin, A.; Zaric, S.; Dai, H. *Nano Res.* **2008**, *1*, 203-212; (d) Wang, H.; Robinson, J.; Li, X.; Dai, H. *J. Am. Chem. Soc.* **2009**, *131*, 9910-9911.
- (10) Eda, G.; Lin, Y.; Mattevi, C.; Yamaguchi, H.; Chen, H.; Chen, I.; Chen, C.; Chhowalla, M. *Adv. Mater.* **2010**, *22*, 505-509.
- (11) L. Xiao, Y. Yang, J. Yin, Q. Li, L. Zhang, *J. Power Sources* **2009**, *194*, 1089-1093.

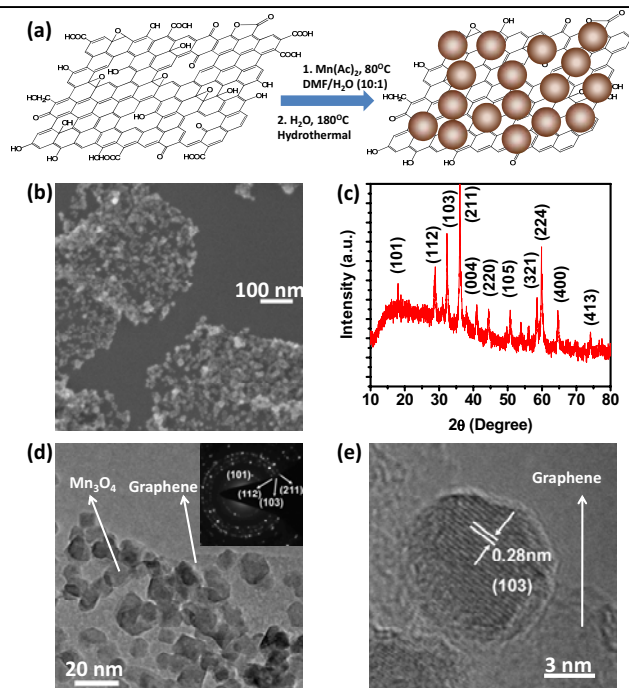


Figure 1. Mn₃O₄ nanoparticles grown on GO. (a) Schematic two-step synthesis of Mn₃O₄/RGO. (b) SEM image of Mn₃O₄/RGO hybrid. (c) XRD spectrum of a packed thick film of Mn₃O₄/RGO. (d) TEM image of Mn₃O₄/RGO, inset shows the electron diffraction pattern of the Mn₃O₄ nanoparticles on RGO. (e) High resolution TEM image of an individual Mn₃O₄ nanoparticle on RGO.

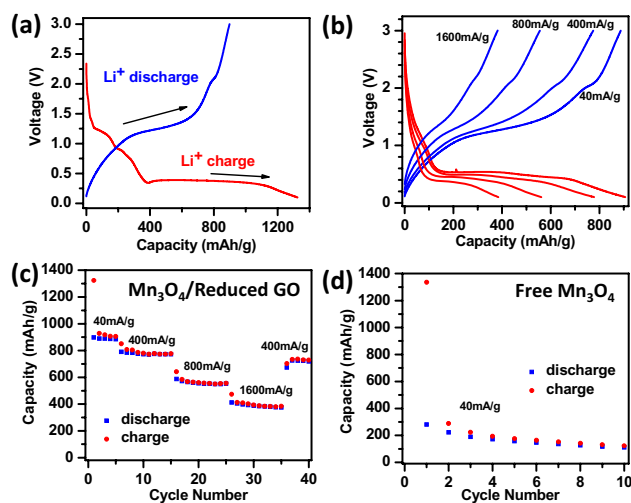


Figure 2. Electrochemical characterizations of a half cell composed of Mn₃O₄/RGO and Li. The specific capacities are based on the mass of Mn₃O₄ in the Mn₃O₄/RGO hybrid. (a) Charge (red) and discharge (blue) curves of Mn₃O₄/RGO for the first cycle at a current density of 40 mA/g. (b) Representative charge (red) and discharge (blue) curves of Mn₃O₄/RGO at various current densities. (c) Capacity retention of Mn₃O₄/RGO at various current densities. (d) Capacity retention of free Mn₃O₄ nanoparticles without graphene at a current density of 40 mA/g.